Available online at www.sciencedirect.com
SCIENCE DIRECT®
Journal of Organometallic Chemistry 683 (2003) 181–190
Journal of Organometallic Chemistry
www.elsevier.com/locate/jorganchem

Theoretical exploration of structure–reactivity relationships in organometallic chemistry: butadiene insertion into the organyl–transition-metal bond and conversion of the allyl–transition-metal fragment in the [Ni^{II}(η^5-Cp)(η^1-phenyl)(η^2-butadiene)] complex

Sven Tobisch *, Rudolf Taube

Institut für Anorganische Chemie der Martin-Luther-Universität Halle-Wittenberg, Fachbereich Chemie, Kurt-Mothes-Straße 2, D-06120 Halle, Germany

Received 2 April 2003; received in revised form 21 June 2003; accepted 23 June 2003

Abstract

We have theoretically examined the reaction course of the butadiene insertion into the aryl–Ni^{II} bond in the [Ni^{II}(η^5-Cp)(η^1-phenyl)(η^2-butadiene)] complex (**1**), by employing a gradient-corrected DFT method. Critical elementary processes have been scrutinized, viz. monomer insertion, rotational allylic isomerization and allylic η^1-$\sigma \rightarrow \eta^3$-$\pi$ rearrangement. The first mechanism suggested by Lehmkuhl et al. was refined and supplemented with important details. The critical factors that determine the generation of *anti*-η^3- and *syn*-η^3-allyl isomers of the [Ni^{II}(η^5-Cp)(1-benzyl-allyl)] product have been elucidated. This let us to rationalize the experimentally observed, almost exclusive formation of the *anti*-η^3-allyl isomer. Butadiene preferably inserts in η^2-mode into the η^1-phenyl–Ni^{II} bond, initially giving rise to the $\eta^1(C^3)$-allyl product species, **3σ**. The direct formation of the η^3-allyl product species, **3π**, along the alternative path for η^4-butadiene insertion, however, is found to be almost entirely disabled kinetically. The thermodynamically favorable η^2-*trans* form of **1** is also shown to be more reactive in accomplishing C–C bond formation. Species **3σ** is indicated to be a metastable intermediate, occurring in an appreciable stationary concentration. Its respective *anti* and *syn* isomeric forms are likely to be in equilibrium, due to the facile rotational isomerization. The subsequent allylic rearrangement into the thermodynamically strongly favorable η^3-allyl–Ni^{II} coordination mode is shown to be the crucial elementary step that discriminates which of the isomeric η^3-allyl forms is preferably generated. The higher reactivity of the *anti* isomer in this process decisively determines the almost exclusive formation of the *anti*-η^3-allyl product species under kinetic control. The requirement of elevated temperatures for the *anti*-η^3-allyl $\rightarrow$ *syn*-η^3-allyl isomerization to occur, as revealed from experiment, is attributed to the pronounced thermodynamic stability of the η^3-allyl–Ni^{II} coordination.

Keywords: Transition-metal allyl complexes; Allylic isomerization; Nickel complexes

1. Introduction

Transition-metal allyl complexes are of outmost importance in organometallic chemistry as they represent real catalysts or reaction intermediates for a number of highly valuable processes in homogeneous catalysis. The transition-metal-assisted conversion processes of 1,3-dienes, with the polymerization, cyclooligomerization and linear oligomerization as prominent examples, are of particular mechanistic interest since they involve the stereoselective formation of a C–C bond. In a series of theoretical investigations, we have provided a comprehensive and detailed mechanistic view of the entire reaction course for the allylnickel(II)-catalyzed [1,2] as well as allyltitanium(III)-catalyzed [3] 1,4-polymerization of 1,3-dienes, and also for the nickel-catalyzed cyclooligomerization of 1,3-butadiene [4,5].

On the basis of our previous theoretical mechanistic exploration of all experimentally verified types of allylnickel(II) catalysts for butadiene polymerization,

* Corresponding author. Tel.: +49-3455525659; fax: +49-3455527028.
E-mail address: tobisch@chemie.uni-halle.de (S. Tobisch).

0022-328X/03/$ - see front matter © 2003 Elsevier B.V. All rights reserved.
doi:10.1016/S0022-328X(03)00596-5

we have been able to establish the operative mechanisms for the critical monomer insertion and allylic isomerization steps of the chain propagation cycle and to elucidate the subtle interplay between these two elementary processes for the regulation of the *cis*–*trans* selectivity of the polymerization reaction. Chain growth proceeds via η^4-*cis*-butadiene insertion into the η^3-butenyl–Ni^{II} bond (π-allyl insertion mechanism [6]), giving rise to the formation of an *anti*-η^3-butenyl group as the growing chain's reactive end under kinetic control. It has been shown that the isomeric *anti* and *syn* forms of the η^3-butenyl–Ni^{II} bond can display a different reactivity when undergoing *cis*-butadiene insertion. Which one of the two forms is more reactive depends on the catalyst's structure, which also has a strong influence on the rate of the interconversion of the initially formed *anti*-η^3-butenyl group into the thermodynamically favorable *syn*-η^3 isomer. For different allylnickel(II) catalysts, the allylic isomerization was found to be either more rapid or slower than butadiene insertion, regardless of whether an individual catalyst promotes the generation of a polybutadiene of predominant *cis*-1,4 or *trans*-1,4 structure.

In order to further enhance the insights into the delicate competition between the 1,3-diene insertion into the organyl–transition-metal bond and the subsequent allylic conversion, we decided to computationally scrutinize the reaction course of the well-characterized butadiene insertion into the aryl–Ni^{II} bond, in the case of the [Ni^{II}(η^5-Cp)(η^1-phenyl)(η^2-butadiene)] complex (cf. Eq. (1)) [7]. Lehmkuhl et al. [7] reported a facile insertion process taking place at low temperature (> -60 °C) that leads exclusively to the *anti*-η^3-allyl form of the [Ni^{II}(η^5-Cp)(1-benzyl-allyl)] product complex. This kinetic insertion product undergoes conversion into the thermodynamically more stable *syn*-η^3-allyl isomer at elevated temperatures (60 °C), which indicates that the insertion step is distinctly more facile than the allylic *syn*–*anti* isomerization.

$$[Ni^{II}(\eta^5\text{-Cp})(\eta^1\text{-phenyl})(\eta^2\text{-}trans\text{-butadiene})] \xrightarrow[-60\ ^\circ C]{} [Ni^{II}(\eta^5\text{-Cp})\{anti\text{-(1-benzyl-}\eta^3\text{-allyl)}\}] \xrightarrow[60\ ^\circ C]{\Delta} [Ni^{II}(\eta^5\text{-Cp})\{syn\text{-(1-benzyl-}\eta^3\text{-allyl)}\}] \quad (1)$$

According to the proposed reaction course [7] (cf. Scheme 1), the C–C bond formation process is envisioned to commence from the thermodynamically preferred η^2-*trans*-butadiene isomer of the π-complex, and proceed with the butadiene insertion in its monodentate coordination mode into the phenyl–Ni^{II} bond, which may initially afford a *syn*-$\eta^1(C^3)$-σ-allyl product species (please note the *syn*–*trans* correlation, vide infra). This σ-allyl intermediate undergoes $\eta^1 \rightarrow \eta^3$ allylic rearrangement to yield the favorable η^3-π-allyl–Ni^{II} configuration. The thermodynamically more stable *syn*-η^3-allyl product isomer is reachable through a direct, but obviously suppressed path, while for generation of the *anti*-η^3 isomer the allylic group first has to isomerize, which is likely to occur via rotation of the vinyl group around the C^2–C^3 single bond. From this tentative reaction course, however, it is not evident why the *anti*-η^3-allyl form is formed as the kinetic reaction product, while the reaction path for the directly accessible thermodynamically more stable *syn*-η^3 isomer remains almost entirely precluded.

To clarify this intriguing mechanistic subject, we will computationally scrutinize the overall reaction course by employing a density functional (DFT)-based method, which has been demonstrated to be reliable for predicting both structural and energetic aspects of transition-

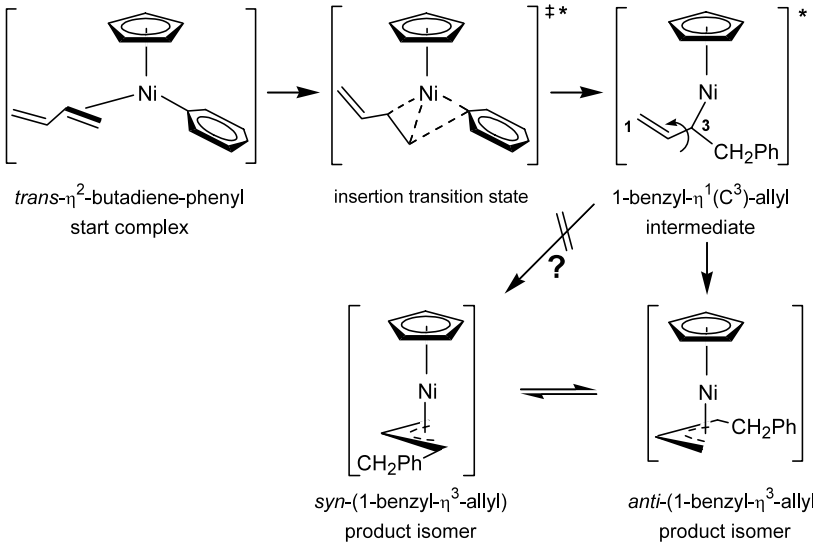

Scheme 1. Proposed reaction course for butadiene insertion into the aryl–Ni^{II} bond occurring in the [Ni^{II}(η^5-Cp)(η^1-phenyl)(η^2-butadiene)] complex [7]. The starred species were postulated to participate along the course for formation of the *anti*-1-benzyl-η^3-allyl kinetic product.

metal complexes. Our examination comprises of the following key elementary steps: (1) the butadiene insertion into the η^1-phenyl–Ni^{II} bond, (2) the interconversion of the two isomeric *anti*- and *syn*-allyl forms and (3) the η^1-$\sigma \rightarrow \eta^3$-$\pi$ rearrangement of the allyl–Ni^{II} fragment. Although the η^2-*trans*-butadiene insertion is suggested as the probable C–C bond formation path [7], one should note that the insertion step exhibits a certain mechanistic diversity. Butadiene insertion gives rise to an *anti*- or *syn*-allyl group in the kinetic product when starting from its s-*cis* or s-*trans* configuration (*anti*−*cis* and *syn*−*trans* correlation), which furthermore can occur with the butadiene coordinated in a monodentate or a bidentate fashion.

The present study is aimed at elucidating the following questions:

1) How does the butadiene insertion preferably proceed? Is the postulated $\eta^1(C^3)$-allyl intermediate involved along the most feasible insertion path, or is there an alternative insertion path that leads directly to η^3-allyl product?
2) How are the isomeric *anti* and *syn* forms of the $\eta^1(C^3)$-σ and η^3-π-allyl–Ni^{II} species of the [Ni^{II}(η^5-Cp)(1-benzyl-allyl)] complex distinguished in their stability and reactivity?
3) Which factors are decisive in determining the almost exclusive formation of an *anti*-η^3-allyl group in the kinetic insertion product?

Addressing these questions will contribute to enhance the understanding of the catalytic structure–reactivity relationships in the C–C bond formation process proceeding by 1,3-diene insertion into the organyl–transition-metal bond.

2. Computational details

2.1. Method

The calculations have been performed at the gradient-corrected DFT level by using the TURBOMOLE program package developed by Häser and coworkers [8]. The local exchange correlation potential by Dirac [9a], Slater [9b] and Vosko et al. [9c] was augmented with gradient-corrected functionals for electron exchange according to Becke [9d] and correlation according to Perdew [9e,9f] in a self-consistent fashion. This gradient-corrected density functional is usually termed BP86 in the literature. In recent benchmark computational studies it was shown that the BP86 functional gives results in excellent agreement with the best wave function-based method available today, for the class of reactions investigated here [10].

For all atoms a standard all-electron basis set of triple-ζ quality for the valence electrons augmented with polarization functions was employed for the geometry optimization and the saddle-point search. The Wachters [11a] 14s/9p/5d set supplemented by two-diffuse p [11b] and one-diffuse d function [11b] contracted to (62111111/5111111/3111) was used for nickel, and standard TZVP basis sets [11c] were employed for carbon (a 10s/6p/1d set contracted to (7111/411/1)) and for hydrogen (a 5s/1p set contracted to (311/1)). The frequency calculations were done by using standard DZVP basis sets [11c], which consist of a 15s/9p/5d set contracted to (63321/531/41) for nickel, a 9s/5p/1d set contracted to (621/41/1) for carbon and a 5s set contracted to (41) for hydrogen, for DZVP optimized structures, which differ in marginal extent from the triple-ζ optimized ones. The corresponding auxiliary basis sets were used for fitting the charge density [11c,11d].

2.2. Stationary points

The geometry optimization and the saddle-point search were carried out at the BP86 level of approximation by utilizing analytical/numerical gradients/Hessians according to standard algorithms. No symmetry constraints were imposed in any case. The stationary points were identified exactly by the curvature of the potential energy surface at these points corresponding to the eigenvalues of the Hessian. All reported transition states possess exactly one negative Hessian eigenvalue, while all other stationary points exhibit positive eigenvalues exclusively. The educt and product that correspond directly to the located transition-state structure were verified by following the reaction pathway going downhill to both sides from slightly relaxed transition-state structures. Reaction and activation free energies (ΔG, $\Delta G^{\ddagger}$ at 298 K and 1 atm) were evaluated according to standard textbook procedures [12] using computed harmonic frequencies.

2.3. Labeling of the molecules

A number of labeling conventions have been adopted throughout this paper. The following arabic numerals were chosen for key species of the reaction course: viz. **1** for the [Ni^{II}(η^5-Cp)(η^1-phenyl)(η^2-butadiene)] π-complex, **2** for the transition state for butadiene insertion into the phenyl–Ni^{II} bond, **3σ** and **3π** for the $\eta^1(C^3)$-σ- and η^3-π-allyl species of the [Ni^{II}(η^5-Cp)(1-benzyl-allyl)] insertion product, **4** for the transition state for rotational allylic isomerization and **5** for the transition state involved in the η^1-$\sigma \rightarrow \eta^3$-$\pi$ allylic rearrangement. The *anti* and *syn* isomers for **3** and **5** were labeled **a** and **s**, respectively, corresponding to isomers of **1** and **2** involved along *cis*-butadiene, i.e. **1c**, **2c**, and *trans*-

butadiene insertion paths, i.e. **1t**, **2t** [13]. The enantiomeric forms of the allyl–Ni^{II} and the butadiene–Ni^{II} coordination are schematically depicted in Fig. 1, which will be denoted according to the commonly used Re/Si terminology [14]. The several isomers that are possible for each of the key species **1**–**5** were carefully explored. The respective enantiomers of **1**–**5** were found to be very close in energy (cf. Table 1); thus, the energetics of neither of the examined elementary steps is remarkably affected by the involved butadiene or allyl enantiofaces.

3. Exploration of crucial elementary processes

We shall start our investigation by examining important elementary processes of the entire C–C bond formation reaction, step by step. The free energies of all relevant key species are collected in Table 1. On the basis of the achieved detailed understanding, the experimental observations will be rationalized by elucidating the factors that determine the formation of the *anti*-η^3-allyl product under kinetic control.

3.1. Butadiene π-complex

Probing different kinds of butadiene coordination revealed that butadiene preferably coordinates in a monodentate fashion. In agreement with the experimental characterization [7], the [Ni^{II}(η^5-Cp)(η^1-phenyl)(η^2-butadiene)] compound (**1**) is the thermodynamically favored form of the π-complex (cf. Fig. 2). Despite several efforts, we have not been able to locate species where the butadiene is coordinated in the bidentate mode. Starting from suitably chosen initial structures and allowing free relaxation, they always arrive to the η^2-butadiene species. On the other hand, when the η^4-butadiene coordination was fixed, then energetically high lying stationary points could be located, characterized by a reduced hapticity of the Cp ligand in order to create an additional coordination site. Although this so-called ring slippage is known as a facile process for several Cp-based complexes [15], it is seen, not unexpectedly, that butadiene as a weak donor is not able to compete for bidentate coordination with the Cp ligand in **1**.

For butadiene to coordinate in a monodentate fashion, the η^2-*trans* mode, **1t**, is energetically preferred by 2.4 kcal mol^{-1} (ΔG) relative to the η^2-*cis* mode, **1c** (cf. Table 1). The stability of the butadiene coordination is influenced to a minor extent by the involved enantioface, which is due to the fact that the butadiene complexation is not affected by remarkable steric interactions with the remaining ligand sphere (cf. Fig. 2). Accordingly, the several isomeric forms of **1**, representing suitable precursors for the insertion step, are likely to be in equilibrium with the η^2-*trans*-butadiene isomers, **1t**, occurring in highest thermodynamic population.

3.2. Butadiene insertion into the η^1-phenyl–Ni^{II} bond

Two principal paths are conceivable for this elementary step. On the one hand, butadiene can be inserted in η^2-mode as suggested by Lehmkuhl et al. [7]. On the other hand, although energetically disfavored in the π-complex, butadiene may coordinate in a bidentate fashion in the vicinity of the transition state, where the phenyl–Ni^{II} bond can be expected to be weakened to a certain extent. The key species of the path for η^2-butadiene insertion, involving either η^2-*trans* or η^2-*cis*-butadiene isomers, are shown in Fig. 2, while Fig. 3 displays the energetically preferred transition state **2c′**

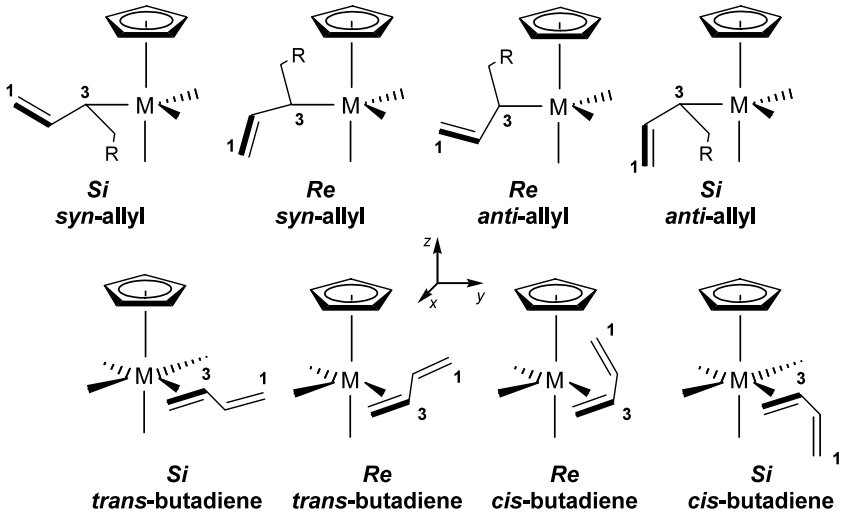

Fig. 1. Two enantiomeric forms of the allyl–transition-metal (*anti* and *syn* configuration, exemplified for the $\eta^1(C^3)$-mode) and the butadiene–transition-metal (s-*cis* and s-*trans* configuration, exemplified for the η^2-mode) coordination [14].

Table 1
Relative Gibbs free energies (ΔG, $\Delta G^{\ddagger}$ in kcal mol^{-1}) of key stationary points involved in crucial elementary steps of the entire reaction course of butadiene insertion into the aryl–Ni^{II} bond to occur in the [Ni^{II}(η^5-Cp)(η^1-C$_6$H$_5$)(η^2-C$_4$H$_6$)] complex [a,b,c]

Category	Description	Species	ΔG,$\Delta G^{\ddagger}$
Butadiene π-complex	η^2-*trans* (Re/Si)	**1t**	0.0/0.9
	η^2-*cis* (Re/Si)	**1c**	2.4/3.6
Insertion TS	η^2-*trans* (Re/Si)	**2t**	17.2/17.1
	η^2-*cis* (Re/Si)	**2c**	18.8/18.8
	η^4-*cis*	**2c′**	30.4
1-Benzyl-η^1(C^3)-allyl product	*syn*-η^1(C^3)-allyl (Re/Si)	**3σs**	0.1/0.1
	anti-η^1(C^3)-allyl (Re/Si)	**3σa**	0.1/−0.2
Rotational allylic isomerization TS	η^1(C^3)-allyl (Re/Si)	**4**	7.9/6.9
η^1(C^3)→η^3 allylic rearranged TS	*syn*-allyl (Re/Si)	**5s**	12.8/12.8
	anti-allyl (Re/Si)	**5a**	10.7/10.7
1-Benzyl-η^3-allyl product	*syn*-η^3-allyl (Re/Si)	**3πs**	−21.8/−21.8
	anti-η^3-allyl (Re/Si)	**3πa**	−20.3/−20.3

[a] Only the most stable isomer for each species is reported.
[b] The two enantiomeric forms of the η^2-butadiene–Ni^{II} and allyl–Ni^{II} coordination are explicitly given (cf. Fig. 1).
[c] Gibbs free energies relative to the most stable isomeric form of [Ni^{II}(η^5-Cp)(η^1-C$_6$H$_5$)(η^2-*trans*-C$_4$H$_6$)] (**1t**).

for η^4-*cis*-butadiene insertion. Similar to both paths, a four-membered transition-state structure is passed through that is characterized by a nearly planar *cis* arrangement of the butadiene's double bond being inserted and the phenyl–Ni^{II} bond. The transition states occur with the emerging C–C bond being at a distance of ∼1.90–2.00 Å, while the phenyl–Ni^{II} bond remains almost intact. The η^4-butadiene coordination in **2c′** is seen to occur at the expense of the Cp–Ni^{II} bond strength, as the hapticity of the Cp ligand changes from η^5 to η^2. Following the reaction paths downhill from the transition states, we find that the η^4-butadiene insertion leads directly to the η^3-allyl product **3π**; thus, the *anti*-η^3-allyl isomer **3πa** is generated from **2c′** [13,16]. In contrast, transition states **2t**, **2c** for η^2-*trans* and η^2-*cis* butadiene insertion decay into the *syn* and *anti* isomers of the η^1(C^3)-allyl product species, **3σs** and **3σa**, respectively [13].

Comparison of the activation free energies for the two alternative paths reveals clearly (cf. Table 1) that the η^4-butadiene insertion does not represent a viable reaction path, since it is predicted to be connected with a barrier of ∼30 kcal mol^{-1} ($\Delta G^{\ddagger}$). This substantial barrier, however, is not consistent with the experimental observation of a facile insertion process (cf. Section 1 [7]). The dominant path for C–C bond formation is the insertion of butadiene in η^2-mode—thus formally as a vinylethylene—into the η^1-phenyl–Ni^{II} bond via **2**,

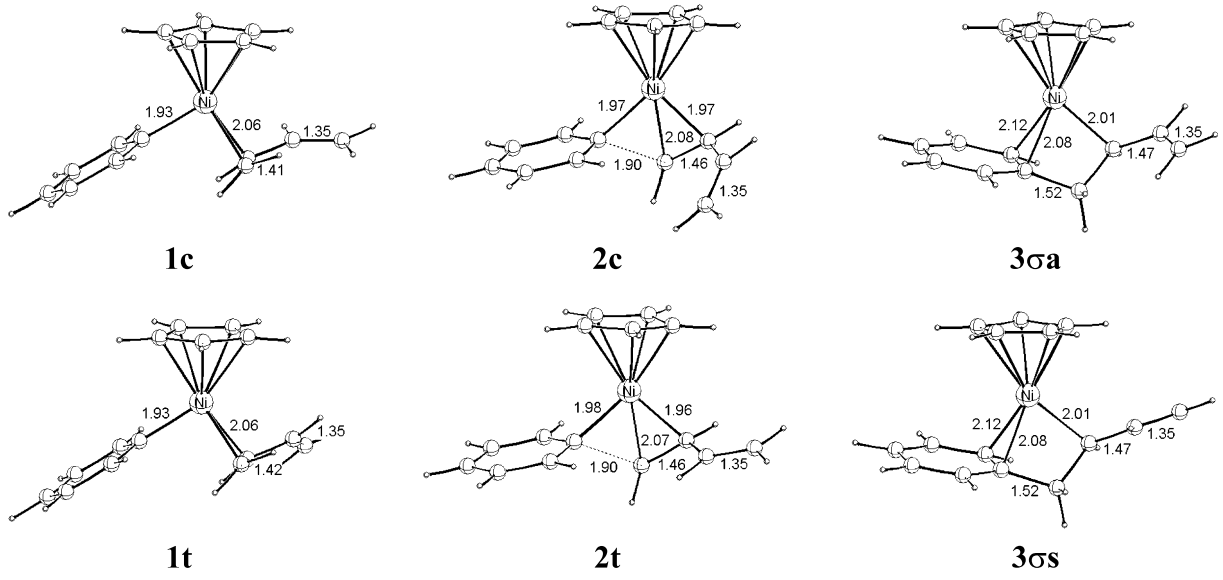

Fig. 2. Butadiene insertion in η^2-mode into the η^1-phenyl–Ni^{II} bond of [Ni^{II}(η^5-Cp)(η^1-phenyl)(η^2-butadiene)] compound (**1**) to afford the [Ni^{II}(η^5-Cp)(1-benzyl-η^1(C^3)-allyl)] species **3σ**. Selected geometric parameters [Å] of the optimized structures of key species are given for insertion to commence from η^2-*trans* and η^2-*cis*-butadiene isomers of **1**.

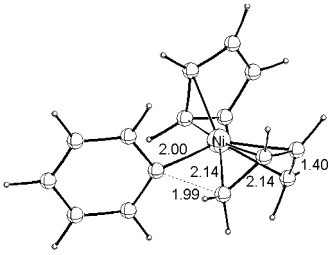

2c'

Fig. 3. Selected geometric parameters [Å] of the optimized structure of transition state **2c**′ for η^4-*cis* butadiene insertion to yield the [Ni^{II}(η^5-Cp){*anti*-(1-benzyl-η^3-allyl)}] species **3πa** [16].

affording the $\eta^1(C^3)$-allyl species **3σ** as the initial product. This path is predicted to be distinctly favored on kinetic considerations due to the activation barrier being more than 10 kcal mol^{-1} ($\Delta\Delta G^{\ddagger}$) lower than that for the entirely precluded path for η^4-butadiene insertion.

Along the preferred **1**→**3σ** insertion path the η^2-butadiene undergoes rotation to achieve the quasi-planar four-membered transition state **2**, where the α-C(phenyl) p-orbital and the olefinic π-system of butadiene can interact most efficiently. The barrier for olefin rotation was determined by experiment to be 12.1 kcal mol^{-1} ($\Delta G^{\ddagger}$) for the related [Ni^{II}(η^5-Cp)(CH_3)(C_2H_4)] complex [17]. Our computed barrier of 12.4 kcal mol^{-1} ($\Delta G^{\ddagger}$) is in excellent agreement with this value and demonstrates the degree of accuracy that can be achieved by the applied computational methodology. For the [Ni^{II}(η^5-Cp)(η^1-phenyl)(η^2-olefin)] type of complexes, the ethylene and η^2-butadiene rotational process is predicted to require very similar barriers, those amount to 11.0 and 11.3 kcal mol^{-1} ($\Delta G^{\ddagger}$, [18]), respectively. The acceleration of the rotational process upon going from the methyl to the phenyl substituent is understandable, since the backbonding contribution to the olefin–Ni^{II} bond becomes reduced for the latter. Interestingly, the butadiene rotation contributes to a major extent to the overall insertion barrier, as revealed from the comparison of the respective barriers for rotation ($\Delta G^{\ddagger} = 11.3$ kcal mol^{-1}) and insertion ($\Delta G^{\ddagger} = 17.1$ kcal mol^{-1}), as exemplified for the η^2-*trans*-butadiene isomer.

The free energy gap between *cis*- and *trans*-butadiene forms in **1** is approximately preserved in **2**, giving rise to almost identical intrinsic barriers for *cis*- and *trans*-butadiene insertion. Furthermore, the involved butadiene's enantioface has a minor influence on the barrier's height. The several isomers of the precursor **1** are, however, likely to be in equilibrium. Accordingly, the probability for the alternative insertion of η^2-*cis*- or η^2-*trans*-butadiene is entirely discriminated by the respective total barriers (i.e. **2c**, **2t**, relative to the most stable isomer of **1**) on account of the Curtin–Hammett principle [19]. In terms of total barriers, butadiene is indicated to preferably insert in η^2-*trans* mode into the η^1-phenyl–Ni^{II} bond via **2t** with an activation barrier of 17.1 kcal mol^{-1} ($\Delta G^{\ddagger}$), while the η^2-*cis*-butadiene insertion is kinetically impeded by a barrier that is 1.7 kcal mol^{-1} ($\Delta\Delta G^{\ddagger}$) higher. Thus, the thermodynamically most stable η^2-*trans* form, **1t**, of the butadiene π-complex is seen to also represent the more reactive precursor species along the favorable **1**→**3σ** insertion path. This leads to the *syn*-$\eta^1(C^3)$-allyl isomer **3σs** being the prevalent initial product, together with a smaller portion of **3σa** (due to the retarded insertion via **1c**→**3σa**), both of which are generated in a nearly thermoneutral process. The $\eta^1(C^3)$-σ-allyl coordination in **3σ** is stabilized by the coordination of the phenyl group's double bond next to the α-C(phenyl) to nickel (cf. Fig. 2). We have explicitly probed whether excess butadiene can act to replace the η^2-phenyl–Ni^{II} coordination. On the potential energy surface (ΔE) the complexation of an additional butadiene moiety, which occurs at the expense of the coordinated phenyl ring, is an exothermic process ($\Delta E \sim -6$ kcal mol^{-1}). This stabilization, however, cannot compensate for the entropic costs associated with butadiene coordination (~ 14 kcal mol^{-1}). Thus, **3σ**, stabilized by η^2-phenyl group's coordination, is the starting point for the subsequently required allylic conversion processes, which will be analyzed next.

3.3. Rotational allylic isomerization

Commencing from the predominantly formed *syn*-$\eta^1(C^3)$ species **3σs** of the insertion step, the interconversion of the allylic moiety into the *anti* isomer is a necessary elementary process along the overall reaction course to yield the *anti*-η^3-allyl product **3πa**. The isomerization of the allylic moiety is most likely to proceed by internal rotation of the vinyl group around the formal C^2–C^3 single bond occurring in a $\eta^1(C^3)$-σ-allyl–transition-metal species. This has been confirmed both by experimental [20] and theoretical evidence [21]. Accordingly, **3σ** is well situated to act as the precursor for allylic isomerization, requiring no further preceding skeletal rearrangements.

The different isomeric forms of the initially generated $\eta^1(C^3)$-allyl species **3σ**, viz. *anti* and *syn* isomers in two enantiomeric forms, are found to be very close in free energy (cf. Table 1). This is due to the fact that in all cases the allylic coordination does not suffer from any noticeable steric interaction with the remaining ligand sphere. According to our previous detailed investigation of the allylic isomerization in allyl–Ni^{II} complexes [21], several pathways for this process have been examined. The favorable isomer of transition state **4** for rotational isomerization of the allylic moiety, which are encountered along the most feasible isomerization pathway, is

displayed in Fig. 4, together with the respective species **3σs** and **3σa**. An activation free energy of 6.9–7.9 kcal mol^{-1} has to be overcome for allylic interconversion of the *syn*-η^1(C^3) isomer into the *anti*-η^1(C^3) counterpart. This indicates the rotational **3σs** → **4** → **3σa** isomerization to be a facile process. Furthermore, this elementary process is not likely being accelerated further by the presence of excess butadiene. Similar to the findings for **3σ**, the rotational transition state **4**, as well, is not found to be stabilized by a possible coordination of additional butadiene.

3.4. Allylic η^1(C^3)-σ → η^3-π rearrangement

The final step of the reaction course towards the formation of the thermodynamically favorable product species **3π** is the η^1(C^3)-σ → η^3-π rearrangement of the allyl–Ni^{II} moiety. The species **3π** is unequivocally characterized as the [Ni^{II}(η^5-Cp)(1-benzyl-η^3-allyl)] compound [7]. In agreement with experiment, the *syn* isomer, **3πs**, is predicted to be thermodynamically favorable relative to the *anti* counterpart **3πa**; the gap amounts to 1.5 kcal mol^{-1} (Δ*G*). The similar stability of η^1(C^3)-allyl isomers **3σa** and **3σs** (cf. Section 3.3), together with the slightly larger thermodynamic driving force for the **3σs** → **3πs** rearrangement relative to the **3σa** → **3πa**, seems to make it unlikely that thermodynamic considerations are decisive for the formation of **3πa** as the kinetic product.

The allylic **3σ** → **3π** rearrangement is accompanied with displacement of the phenyl ring, that is η^2-coordinated in **3σ**; thus, this process is unlikely to proceed in a barrierless fashion. The potential energy surface was scanned in a detailed manner, but without taking species characterized by a strongly distorted Cp–Ni^{II} coordination into explicit consideration. As demonstrated in former sections, these species with a reduced hapticity of the Cp ligand are very unlikely to participate along any viable pathway. Two energetically close lying conformations of the respective transition state **5** have been located that differ in the orientation of the phenyl ring; the favorable of which is displayed in Fig. 5 for *anti*- and *syn*-allyl isomers. The transition state **5** for η^1(C^3)-σ → η^3-π allylic rearrangement is characterized by a partly preformed π-allyl moiety, which is approximately halfway between **3σ** and **3π**, together with a substantially weakened η^2-phenyl–Ni^{II} coordination. Thus, **5** constitutes the phenyl group's displacement by the emerging η^3-allyl–Ni^{II} moiety occurring in a concerted fashion. This process is driven by a strong, but similar thermodynamic force (Δ*G* = −20.1 and −21.9 kcal mol^{-1} for **3σa** → **3πa** and **3σs** → **3πs**, respectively) for the *anti* and *syn* isomers. In contrast, the two isomeric forms exhibit a different reactivity in undergoing allylic η^1(C^3) → η^3 rearrangement. Commencing from **3σa**, the *anti*-η^3-allyl species **3πa** is formed after crossing **5a** with a barrier of 10.9 kcal mol^{-1} (Δ*G*‡), while the activation free energy for the **3σs** → **5s** → **3πs** process amounts to 12.7 kcal mol^{-1}. This indicates the allylic η^1(C^3)-σ → η^3-π rearrangement as a smooth process with a moderate kinetic barrier, that is more facile for the *anti* isomer when compared with the *syn* counterpart.

4. Entire view on the C–C bond formation process

Having inspected critical elementary steps we are now in the position to provide a detailed view of the entire reaction course for the butadiene insertion into the η^1-phenyl–Ni^{II} bond in the [Ni^{II}(η^5-Cp)(η^1-phenyl)(η^2-butadiene)] complex (**1**), the free energy profile of which is presented in Scheme 2.

The several isomeric forms of **1** exist in equilibrium, where the η^2-*trans* form **1t** is prevalent, together with a lower concentration of the η^2-*cis* congener **1c**. The butadiene preferably inserts in η^2-mode, thus formally as vinylethylene, into the η^1-phenyl–Ni^{II} bond to afford initially the η^1(C^3)-σ-allyl species **3σ** in a nearly thermoneutral process. The thermodynamically favorable η^2-*trans* form **1t** is shown to be also more reactive in accomplishing C–C bond formation. Crossing **2t** with a barrier of 17.1 kcal mol^{-1} (Δ*G*‡) leads to the *syn*-η^1(C^3) isomer **3σs** as the predominant initial product, while the generation of **3σa** is kinetically impeded by a total activation barrier, that is 1.7 kcal mol^{-1} (ΔΔ*G*‡) larger. The alternative η^4-butadiene insertion path, that would give rise directly to the η^3-allyl product species **3π**

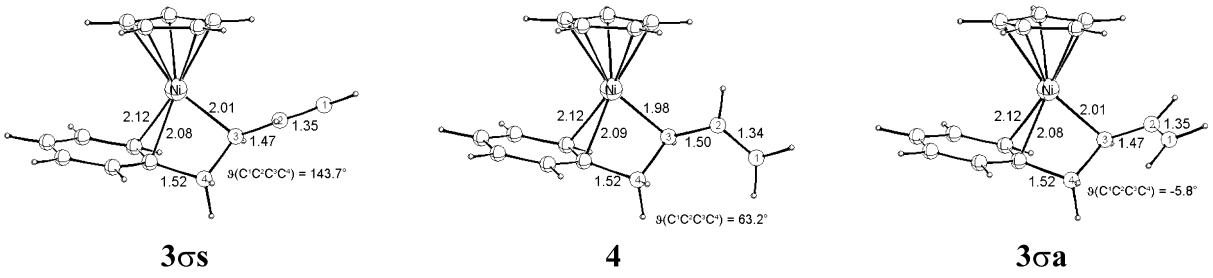

Fig. 4. Rotational allylic isomerization occurring in the [Ni^{II}(η^5-Cp)(1-benzyl-η^1(C^3)-allyl)] species **3σ**. Selected geometric parameters [Å] of the optimized structures of key species are given.

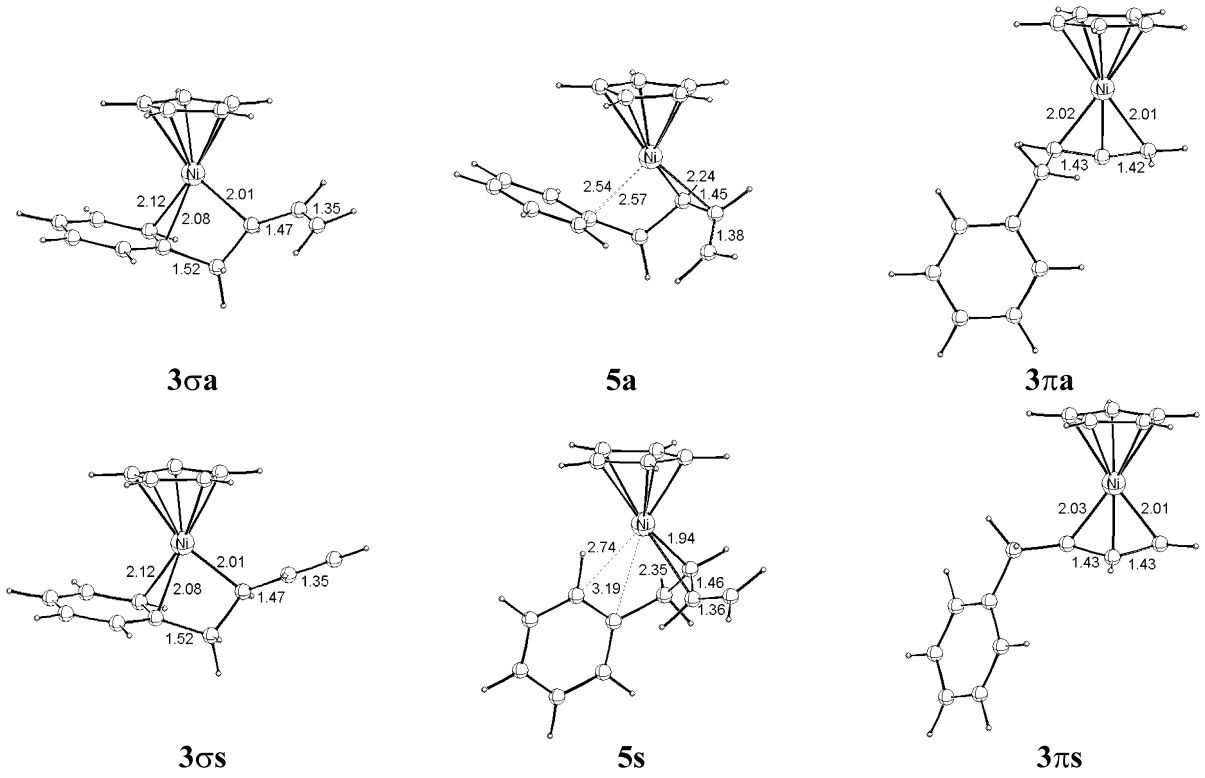

Fig. 5. $\eta^1(C^3)$-$\sigma \rightarrow \eta^3$-$\pi$ rearrangement of the allyl–Ni^{II} fragment in the [$Ni^{II}(\eta^5$-Cp)(1-benzyl-allyl)] product. Selected geometric parameters [Å] of the optimized structures of key species are given for *syn*- and *anti*-allyl isomers.

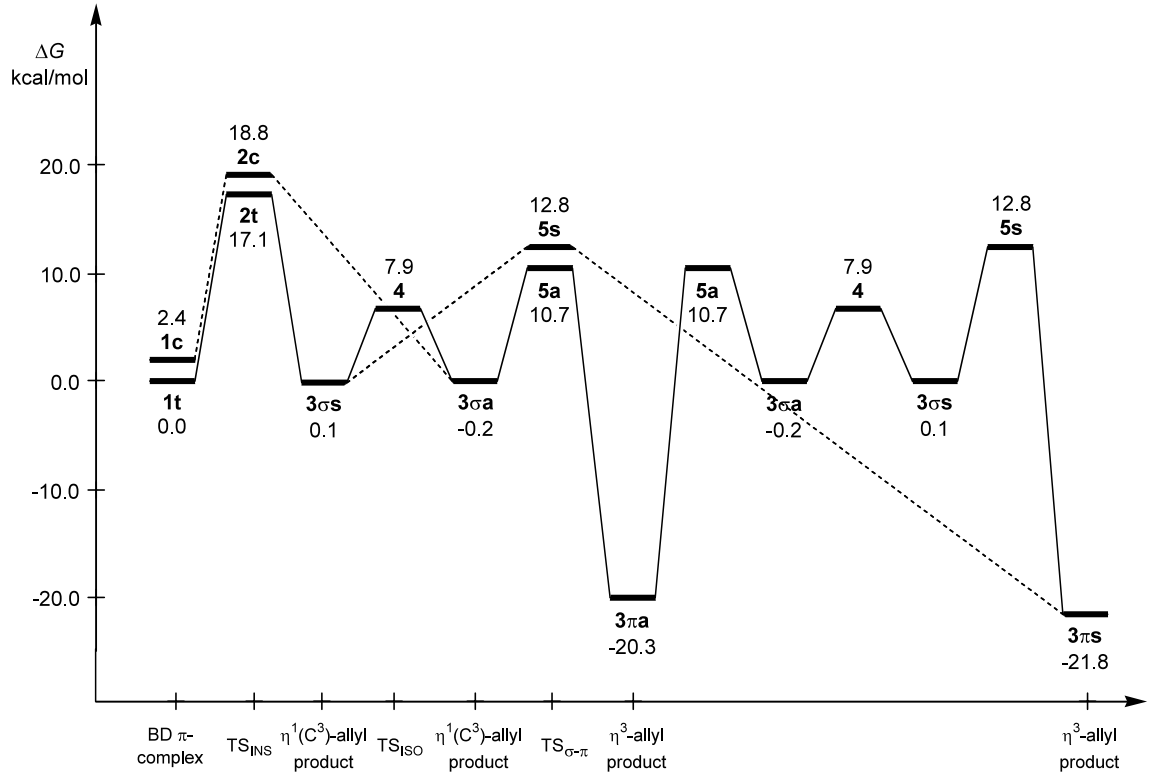

Scheme 2. Gibbs free energy profile (kcal mol^{-1}) of crucial elementary steps of the entire reaction course for η^2-butadiene insertion into the aryl–Ni^{II} bond occurring in the [$Ni^{II}(\eta^5$-Cp)(η^1-C_6H_5)(η^2-C_4H_6)] complex. Unfavorable pathways of individual steps are indicated by dashed lines.

in a strongly exergonic and therefore thermodynamically preferred process, however, is almost entirely disabled on kinetic considerations due to a distinct higher barrier ($\Delta\Delta G^{\ddagger} > 10$ kcal mol^{-1}).

Commencing from the predominantly formed *syn*-$\eta^1(C^3)$-allyl species **3σs** a different sequence of elementary steps is followed to afford the η^3-allyl species **3πs** and **3πa**, respectively. Allylic $\eta^1(C^3)$-σ → η^3-π rearrangement leads to **3πs**, while allylic isomerization is required as a preceding step for generation of **3πa**. The *syn*–*anti* **3σs** → **4** → **3σa** rotational isomerization is indicated to be the most facile of all the elementary steps, having a barrier of 6.8–7.8 kcal mol^{-1} ($\Delta G^{\ddagger}$, relative to **3σs**). On the other hand, for allylic **3σ** → **3π** rearrangement to cross transition state **5**, a barrier has to be overcome, which is at least 3.8 kcal mol^{-1} larger ($\Delta\Delta G^{\ddagger}$). Accordingly, **3σ** represents a metastable intermediate that should occur in an appreciable stationary concentration (although not detectable by NMR [7]), since **3σ** is separated by significant, but moderate barriers from **1** and **3π** ($\Delta G^{\ddagger} = 17$ kcal mol^{-1} for **3σs** → **1t** and 10.9 kcal mol^{-1} for **3σa** → **3π**). The isomeric forms of **3σ**, that are found to be close in energy, are likely to be in a kinetically mobile, dynamic equilibrium, due to the facile rotational isomerization. Therefore, the thermodynamic population of **3σs** and **3σa** is given by their relative stabilities, thus suggesting that both occur in similar concentrations.

Commencing from a rapid equilibrium between *anti* and *syn* isomers of **3σ**, the $\eta^1(C^1)$-σ → η^3-π rearrangement of the allyl–Ni^{II} fragment is shown to be the crucial elementary step that determines which of the isomers of **3π** is preferably generated. The reactivity of *anti* and *syn* isomers in accomplishing allylic **3σ** → **3π** arrangement is critical in this regard, and not their respective, although similar, thermodynamic concentrations, on account of the Curtin–Hammett principle [19]. The conversion of the allyl–Ni^{II} fragment into the highly favorable η^3-π coordination mode is a more facile process for the *anti* isomer (via **5a**) than for the *syn* counterpart (via **5s**). The predicted difference in the respective activation free energies of 2.1 kcal mol^{-1} ($\Delta\Delta G^{\ddagger}$) rationalizes the almost exclusive formation of the *anti* isomer **3πa** as the kinetic product of the C–C bond formation process.

Having **3πa** formed in an overall strongly exergonic process ($\Delta G = -20.3$ kcal mol^{-1}, **1t** → **3πa**), with a total moderate barrier of 17.1 kcal mol^{-1} ($\Delta G^{\ddagger}$, **1t** → **3σs**), the interconversion into the more stable *syn*-η^3 isomer **3πs** proceeds through transition state **4** for rotational isomerization. This, however, first requires the **3πa** → **5a** → **3σa** allylic rearrangement with a free energy barrier of 31 kcal mol^{-1}, followed by **3σa** → **4** → **3σs** rotational isomerization ($\Delta G^{\ddagger} = 8.1$ kcal mol^{-1}) and subsequent η^3-π-allyl recreation via **3σs** → **5s** → **3πs** ($\Delta G^{\ddagger} = 12.7$ kcal mol^{-1}) to yield the *syn*-η^3-allyl product species. Thus, allylic *anti*–*syn* isomerization of the thermodynamically favorable η^3-allyl product species requires an overall largest free energy barrier of 33.1 kcal mol^{-1}, which is significantly higher than that for **1t** → **3πa** ($\Delta\Delta G^{\ddagger} = 13.9$ kcal mol^{-1}). This suggests more severe reaction conditions (i.e. elevated temperature) for the first process when compared with the latter, which is consistent with the experimental observation (cf. Section 1 [7]).

5. Summary

We have presented a theoretical mechanistic study of the experimentally well-characterized butadiene insertion into the aryl–Ni^{II} bond occurring in the [Ni^{II}(η^5-Cp)(η^1-phenyl)(η^2-butadiene)] complex (**1**), by employing a gradient-corrected DFT method. The investigation comprises the following crucial elementary processes, viz. monomer insertion, rotational allylic isomerization and allylic η^1-σ → η^3-π rearrangement. The first mechanism proposed by Lehmkuhl et al. [7] has been theoretically refined and supplemented by the following aspects:

1) The several isomeric forms of **1** exist in equilibrium, where the η^2-*trans* form **1t** is prevalent. Butadiene is most likely to insert in η^2-mode into the η^1-phenyl–Ni^{II} bond, giving rise initially to the $\eta^1(C^3)$-allyl species, **3σ**, of the [Ni^{II}(η^5-Cp)(1-benzyl-allyl)] product. The direct formation of the η^3-allyl product species, **3π**, along the alternative path for η^4-butadiene insertion, however, is found to be almost entirely disabled on kinetic considerations. The thermodynamically favorable η^2-*trans* form **1t** is shown to be also more reactive in accomplishing C–C bond formation, thus leading predominantly to the *syn*-$\eta^1(C^3)$ isomer **3σs** in a nearly thermoneutral process. The barrier for this amounts to 17.1 kcal mol^{-1} ($\Delta G^{\ddagger}$).
2) Concerning the [Ni^{II}(η^5-Cp)(1-benzyl-allyl)] product, the $\eta^1(C^3)$-σ-allyl mode, although stabilized by a η^2-phenyl ring's coordination to nickel, is predicted to be thermodynamically significantly less favorable relative to the η^3-π mode of the allyl–Ni^{II} coordination (ΔG(**3π**–**3σ**) > 20 kcal mol^{-1}). The *anti*- and *syn*-$\eta^1(C^3)$-allyl isomers exhibit a very similar thermodynamic stability, while for the η^3-allyl–Ni^{II} coordination, in agreement with experiment, the *syn* form is seen to be preferred (ΔG(**3πs**–**3πa**) = 1.5 kcal mol^{-1}).
3) The initially generated species **3σ** is indicated to be a metastable intermediate that occurs in appreciable stationary concentration. The *anti* and *syn* isomers are likely to be in equilibrium, due to the facile rotational **3σs** → **4** → **3σa** isomerization, which is the

most rapid of all crucial elementary steps of the reaction course.

4) The $\eta^1(C^3)$-$\sigma \rightarrow \eta^3$-$\pi$ rearrangement of the allyl–Ni^{II} moiety, which occurs in a strongly exergonic process with a moderate barrier accompanied, is shown to be the crucial elementary step that discriminates which of the η^3-allyl product isomers is preferably generated. The higher reactivity of the *anti* isomer in this process decisively determines the almost exclusive formation of the *anti*-η^3-allyl product species under kinetic control, while the slower **3σs → 3πs** process prevents the occurrence of the *syn*-η^3-allyl product isomer.
5) The experimental observation that elevated temperatures are necessary for the *anti*-η^3-allyl → *syn*-η^3-allyl isomerization is attributed to the pronounced thermodynamic stability of the η^3-allyl–Ni^{II} coordination.

References

[1] (a) S. Tobisch, H. Bögel, R. Taube, Organometallics 15 (1996) 3563;
(b) S. Tobisch, H. Bögel, R. Taube, Organometallics 17 (1998) 1177;
(c) S. Tobisch, R. Taube, Organometallics 18 (1999) 5204;
(d) S. Tobisch, R. Taube, Chem. Eur. J. 7 (2001) 3681;
(e) S. Tobisch, Chem. Eur. J. 8 (2002) 4756.

[2] S. Tobisch, Acc. Chem. Res. 35 (2002) 96.

[3] S. Tobisch, Organometallics 22 (2003) 2729.

[4] (a) S. Tobisch, T. Ziegler, J. Am. Chem. Soc. 124 (2002) 4881;
(b) S. Tobisch, T. Ziegler, J. Am. Chem. Soc. 124 (2002) 13290;
(c) S. Tobisch, Chem. Eur. J. 9 (2003) 1217.

[5] S. Tobisch, Adv. Organomet. Chem. 49 (2003) 167.

[6] (a) R. Taube, G. Sylvester, in: B. Cornils, W.A. Herrmann (Eds.), Applied Homogeneous Catalysis with Organometallic Compounds, VCH, Weinheim, Germany, 2002, p. 285;
(b) R. Taube, J.-P. Gehrke, P. Böhme, Z. Wiss, Tech. Hochsch. Leuna-Merseburg. 39 (1987) 310;
(c) R. Taube, U. Schmidt, J.-P. Gehrke, P. Böhme, J. Langlotz, S. Wache, Makromol. Chem. Makromol. Symp. 66 (1993) 245;
(d) R. Taube, in: W. Kaminsky (Ed.), Metalorganic Catalysts for Synthesis and Polymerization, Springer, Berlin, Heidelberg, 1999, p. 531.

[7] H. Lehmkuhl, T. Keil, R. Benn, A. Rufinska, C. Krüger, J. Poplawska, M. Bellenbaum, Chem. Ber. 121 (1988) 1931.

[8] (a) R. Ahlrichs, M. Bär, M. Häser, H. Horn, C. Kölmel, Chem. Phys. Lett. 162 (1989) 165;
(b) O. Treutler, R. Ahlrichs, J. Chem. Phys. 102 (1995) 346;
(c) K. Eichkorn, O. Treutler, H. Öhm, M. Häser, R. Ahlrichs, Chem. Phys. Lett. 242 (1995) 652.

[9] (a) P.A.M. Dirac, Proc. Cambridge Philos. Soc. 26 (1930) 376;
(b) J.C. Slater, Phys. Rev. 81 (1951) 385;
(c) S.H. Vosko, L. Wilk, M. Nussiar, Can. J. Phys. 58 (1980) 1200;
(d) A.D. Becke, Phys. Rev. A 38 (1988) 3098;
(e) J.P. Perdew, Phys. Rev. B 33 (1986) 8822;
(f) J.P. Perdew, Phys. Rev. B 34 (1986) 7406.

[10] (a) F. Bernardi, A. Bottoni, M. Calcinari, I. Rossi, M.A. Robb, J. Phys. Chem. 101 (1997) 6310;
(b) V.R. Jensen, K. Børve, J. Comput. Chem. 19 (1998) 947.

[11] (a) A.H.J. Wachters, J. Chem. Phys. 52 (1970) 1033;
(b) P.J. Hay, J. Chem. Phys. 66 (1977) 4377;
(c) N. Godbout, D.R. Salahub, J. Andzelm, E. Wimmer, Can. J. Chem. 70 (1992) 560;
(d) TURBOMOLE Basis Set Library.

[12] D.A. McQuarrie, Statistical Thermodynamics, Harper & Row, New York, 1973.

[13] Please note the *anti-cis* and *syn-trans* correlation, according to which an *anti* or *syn* allylic group is generated as the kinetic product of the C–C bond formation process for butadiene insertion to occur from its s-*cis* or s-*trans* configuration. This relates to the principle of least structure variation and has been verified theoretically by following the reaction path.

[14] (a) K.R. Hanson, J. Am. Chem. Soc. 88 (1966) 2731;
(b) The Re/Si terminology is applied with regard to the chirality of the C^3-atom of the butenyl group and of butadiene (cf. Fig. 1).

[15] see for instance: J.M. O'Connor, C.P. Casey, Chem. Rev. 87 (1987) 307.

[16] The transition state for η^4-*trans*-butadiene insertion into the η^1-phenyl–Ni^{II} bond, **2t′**, could not be located. This would gives rise in a direct way to the *syn*-η^3-allyl product isomer **3πs**, which is expected to require a higher kinetic barrier than for the direct **3πa** formation via **2c′**.

[17] H. Lehmkuhl, in: A. de Meijere, H. tom Dieck (Eds.), Organometallics in Organic Synthesis, Springer, Berlin, Heidelberg, 1987, p. 185.

[18] This value corresponds to the rotation of η^2-*trans*-butadiene in **1t**.

[19] (a) J.I. Seemann, Chem. Rev. 83 (1983) 83;
(b) J.I. Seemann, J. Chem. Educ. 63 (1986) 42.

[20] (a) J.W. Faller, M.E. Thomsen, M.J. Mattina, J. Am. Chem. Soc. 93 (1971) 2642;
(b) J. Lukas, P.W.N.M. van Leeuwen, H.C. Volger, A.P. Kouwenhoven, J. Organomet. Chem. 47 (1973) 153;
(c) K. Vrieze, in: L.M. Jackman, F.A. Cotton (Eds.), Dynamic Nuclear Magnetic Resonance Spectroscopy, Academic Press, New York, 1975, p. 441.

[21] S. Tobisch, R. Taube, Organometallics 18 (1999) 3045.